Optimization of a Rankine Cycle integrated in a Long-Range Intercity Bus with Expander Sizing

Patrick Hadamitzky[1]*, Maximilian Hebeler[2], Jürgen Köhler[2], Roland Scharf[1]

[1]*Leibniz Universität Hannover, Institut für Kraftwerkstechnik und Wärmeübertragung,*
An der Universität 1, 30823 Garbsen, Deutschland
hadamitzky@ikw.uni-hannover.de

[2]*Technische Universität Braunschweig, Institut für Thermodynamik,*
Hans-Sommer-Straße 5, 38106 Braunschweig, Deutschland
m.hebeler@tu-braunschweig.de

*Corresponding author

ABSTRACT

In this work an optimization of a Rankine cycle, nested into a long-range intercity bus for the recovery of exhaust gas exergy is carried out. In order to optimize WHR-systems, it is of great importance to carry out a holistic optimization of the system in combination with all its subsystems and components. The applied working fluid is cyclopentane and the expander design is of scroll type. The main contributors to efficiency changes are the expansion machine and the heat exchangers. As can be seen in the literature, the process optimization is often carried out by assuming a constant efficiency of the expansion machine. If this is done, the relationship between the thermodynamic points of state applied to the in- and outlet of the expander and its efficiency is neglected. Thus, the full optimization potential of the process remains unused and leads to a non-realistic behaviour of the expander. In this paper a holistic approach to optimize the expansion machine and the thermodynamic process states is presented. The optimization is carried out by using accurate thermophysical properties of the working fluid. Part of this optimization is a novel approach to enable the scalability of the expander. The basis is a semi-empirical model well-known in the literature. This model allows the prediction of the expander performance in a wide operating range. To enable the optimization of the sizing of the expander, the model parameters are scaled based on the geometry and selected characteristic numbers. A stationary optimization is carried out. Thanks to its reasonable computational effort of the modelling approaches, an application in transient optimizations is feasible in future works.

1   INTRODUCTION

Space provided in vehicles is highly demanded. Therefore, a successful implementation of a Rankine cycle into the long-range intercity bus requires an appropriate sizing of the components. On the one hand high efficiency is desired. On the other hand, thermodynamic ideal systems yield in large components and complex systems with a negative impact on the efficiency and the operability of the omnibus. An optimization process can be a suitable tool to obtain a solution for the conflicting goals. The expander is a main contributor to the losses inside the Rankine cycle. If the expander is not properly designed, the result might be a severe reduction of the overall system efficiency. Complex physical models of expanders e.g. shown in Ma et al. (2017) or Wu et al. (2015) are cumbersome and computationally expensive. An integration into a holistic optimization approach for the design of a Rankine cycle is complicated and convergence is difficult to achieve. To mitigate these challenges a novel approach is developed. The base model is a loss based expander model of a scroll expander with a more extensive physical background than the most models used in the literature for such optimization approaches. This base model still lacks of a geometrical binding. Without additional constraints, it is not suitable for geometrical scaling in the optimization process. A scaling method is developed to receive a binding to the changes of the expander scroll-geometry. This method is applied to scale the parameters in the base model.

2 RANKINE CYCLE

The investigated Rankine cycle is shown in Figure 1. It consists of a pump, an evaporator, the scroll expander, an internal heat exchanger, and a condenser with a subcooling part. The evaporator is supplied with exhaust gas to evaporate the working fluid. The condenser is cooled by ambient air. It consists of the air cooler 1 to liquify the working fluid and the air cooler 2 for the subcooling. The pressure in state 1 is regulated by a PI-controller by setting the speed of fan 1 and another PI-controller sets the speed of fan 2 and thus controls the subcooling of the working fluid. Through the speed of the pump the degree of overheating in front of the expander is controlled by means of another PI-controller. A final PI-controller sets the expander speed and thus controls the pressure in state 3. The PI-controllers are only shown for the completeness and understanding of the real cycle, but are not of interest for steady state operation.
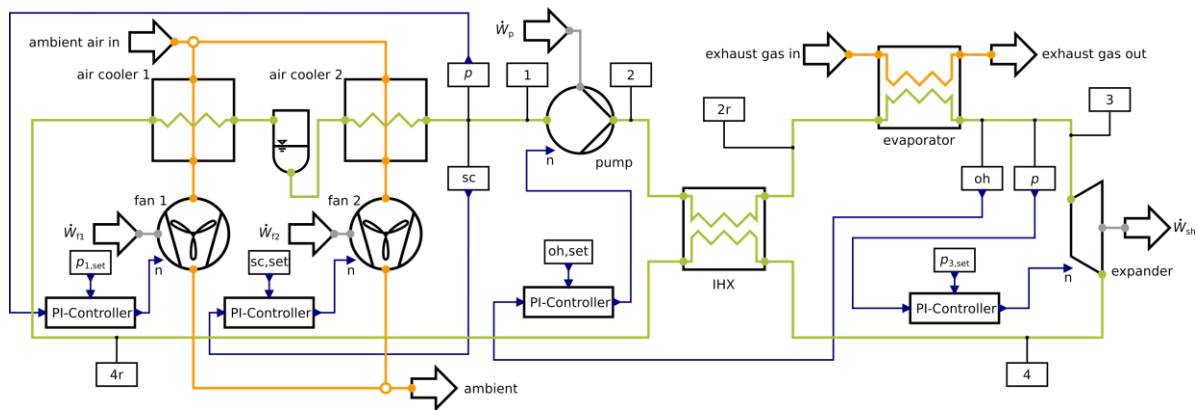

Figure 1: Schematic Overview of the modelled Rankine cycle

3 SIMULATION MODEL

3.1 Rankine cycle

The Rankine cycle described in Chapter 2 is composed of different components of which the most important ones will be described in their modelling. The net power output is given as

$$\dot{W}_{\text{res}} = \dot{W}_{\text{sh}} - \dot{W}_{\text{p}} - \dot{W}_{\text{f1}} - \dot{W}_{\text{f2}}. \tag{1}$$

The modelling approach for the pump and the fans is efficiency based and the shaft power is calculated with a given constant isentropic efficiency by

$$\dot{W} = \frac{1}{\eta_{\text{is}}} \dot{V} \Delta p. \tag{2}$$

The heat exchangers are modeled as fin and tube types, using a finite volume approach. An exhaustive description of the modelling approaches is out of the scope of this paper, but can be found in Kaiser (2020) . The modelling of the expander is based on a well-known approach, as shown in Chapter 3.2, but altered to allow for scaling of the end involute angle ϕ_{e} and thus the volume ratio Π_{E}, as shown in Chapter 3.3.

3.2 Expander

The model on which the scaling method is applied, is the semi-empirical model depicted in Figure 2, which is derived from the model described in Lemort et al. (2009). Models that are similar or even derived from Lemort et al. (2009) are popular and can also be found in more recent literature (e.g. Panesar and Bernagozzi (2019), Fanelli et al. (2018), Ayachi et al. (2016)). The following changes of state of the working fluid are considered in the model as described in Lemort et al. (2009):

su → su, 1:   Adiabatic and isenthalpic pressure drop[1]

su, 1 → su, 2:   Isobaric heat transfer

su, 2 → thr, l: Isentropic pressure drop of the leakage mass flow

su, 2 → ad: Isentropic expansion up to the internal volume ratio, transfer of technical work to the orbiting expander shell

ad → ex, 2:   Accounting for under- or over-expansion: performing the difference of work that is needed for exhausting the volume V_{ad} at the pressure p_{ad} in relation to the pressure $p_{ex,2}$ (see Winandy et al. (2002))

→ ex, 1:   Mixing of the mass flows $\dot{m}_{in}$ and $\dot{m}_{leak}$

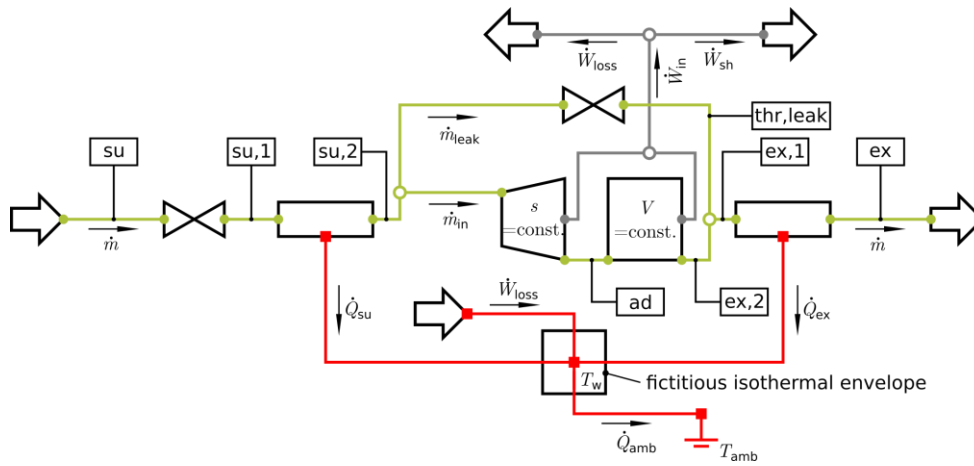ex, 1 → ex: Isobaric heat transfer

Figure 2: Conceptual scheme of the expander model

The system of equations for the calculation of the state variables is shown in Table 1.

Table 1: System of equations for the calculation of the state variables inside the model. Herein means $f(x, y)$ the solution of the equation of state of the unknown state variable. The mass flow $\dot{m}$ and the values in the grey shaded table blocks are given values. The localization i of the state points is shown in Figure 2.

i	p_i	h_i	s_i	ϱ_i	ϑ_i
su	p_{su}	h_{su}	$f(p_{su}, h_{su})$	$f(p_{su}, h_{su})$	$f(p_{su}, h_{su})$
su, 1	$p_{su} - \dfrac{1}{2\varrho_{su}}\left(\dfrac{\dot{m}}{A_{sup}}\right)^2$	h_{su}	$f(p_{su,1}, h_{su,1})$	$f(p_{su,1}, h_{su,1})$	$f(p_{su,1}, h_{su,1})$
su, 2	$p_{su,1}$	$h_{su,1} - \dfrac{\dot{Q}_{su}}{\dot{m}}$	$f(p_{su,2}, h_{su,2})$	$f(p_{su,2}, h_{su,2})$	$f(p_{su,2}, h_{su,2})$
thr, l	$\max(p_{ex,2}, p_{crit,leak})$	$f(p_{thr,l}, s_{thr,l})$	$s_{su,2}$	$f(p_{thr,l}, h_{thr,l})$	$f(p_{thr,l}, h_{thr,l})$
ad	$f(s_{ad}, \varrho_{ad})$	$f(s_{ad}, \varrho_{ad})$	$s_{su,2}$	$\varrho_{ad} = \varrho_{su,2}\dfrac{1}{\Pi_E}$	$f(s_{ad}, \varrho_{ad})$
ex, 2	p_{ex}	$h_{ad} - \dfrac{1}{\varrho_{ad}}(p_{ad} - p_{ex,2})$	$f(p_{ex,2}, h_{ex,2})$	$f(p_{ex,2}, h_{ex,2})$	$f(p_{ex,2}, h_{ex,2})$
ex, 1	p_{ex}	$\dfrac{\dot{m}_{leak}h_{su,2} + \dot{m}_{in}h_{ex,2}}{\dot{m}}$	$f(p_{ex,1}, h_{ex,1})$	$f(p_{ex,1}, h_{ex,1})$	$f(p_{ex,1}, h_{ex,1})$
ex	p_{ex}	$h_{ex,1} - \dfrac{\dot{Q}_{ex}}{\dot{m}}$	$f(p_{ex}, h_{ex})$	$f(p_{ex}, h_{ex})$	$f(p_{ex}, h_{ex})$

---

[1] The modeling of the pressure drop is changed compared with Lemort et al. (2009) from an isentropic to an isenthalpic one because the authors consider it as a more physical plausible modelling approach.

The first law of thermodynamics leads to the following equation for the energy balance of the fictitious isothermal envelope with the temperature T_w

$$0 = \dot{W}_\mathrm{loss} + \dot{Q}_\mathrm{su} + \dot{Q}_\mathrm{ex} - \dot{Q}_\mathrm{amb}, \tag{3}$$

with the heat flux $\dot{Q}_\mathrm{amb}$ given through

$$\dot{Q}_\mathrm{amb} = \alpha_\mathrm{amb} A_\mathrm{amb}(T_\mathrm{w} - T_\mathrm{amb}). \tag{4}$$

The heat transfer occurring in su, $1 \rightarrow$ su, 2 and ex, $1 \rightarrow$ ex is described with the equation

$$\dot{Q}_i = c_{p,i}(\vartheta_i - \vartheta_\mathrm{w})\left(1 - e^{-\frac{kA_i}{\dot{m}c_{p,i}}}\right). \tag{5}$$

It is derived from the integration of the temperature difference of a fluid flow over a heat transfer area with constant surface temperature. The mass flow rate $\dot{m}$ entering the machine is composed of the leakage mass flow rate through the scroll geometry $\dot{m}_\mathrm{leak}$ and the mass flow passing through the scroll under ideal conditions $\dot{m}_{in}$

$$\dot{m} = \dot{m}_\mathrm{in} + \dot{m}_\mathrm{leak}. \tag{6}$$

The mass flow $\dot{m}_\mathrm{in}$ is quantified through the suction volume $V_\mathrm{s,exp}$, the revolutions per time N, and the density $\varrho_\mathrm{su,2}$ adjacent to the suction port of the scroll shells

$$\dot{m}_\mathrm{in} = NV_\mathrm{s,exp}\varrho_\mathrm{su,2}. \tag{7}$$

The leakage mass flow through the scroll geometry is calculated with

$$\dot{m}_\mathrm{leak} = A_\mathrm{leak}\varrho_\mathrm{thr,l}\sqrt{2(h_\mathrm{su,2} - h_\mathrm{thr,l})}, \tag{8}$$

while a mass flow limit by reaching a certain pressure ratio is to consider

$$p_\mathrm{crit,leak} = p_\mathrm{su,2}\left(\frac{2}{\gamma + 1}\right)^{\frac{\gamma}{\gamma - 1}}. \tag{9}$$

The power $\dot{W}_\mathrm{in}$ delivered between su, $2 \rightarrow$ ex, 2 is given through

$$\dot{W}_\mathrm{in} = \dot{m}_\mathrm{in}(h_\mathrm{su,2} - h_\mathrm{ad}) + \dot{m}_\mathrm{in}(h_\mathrm{ad} - h_\mathrm{ex,2}). \tag{10}$$

Reduced by the losses $\dot{W}_\mathrm{loss}$, the power $\dot{W}_\mathrm{sh}$ is received

$$\dot{W}_\mathrm{sh} = \dot{W}_\mathrm{in} - \dot{W}_\mathrm{loss} = \dot{W}_\mathrm{in} - 2\pi N T_\mathrm{loss}.$$

The model is characterized by the 9 parameters shown in Table 2 with the values given in Lemort et al. (2009). Those parameters have to be altered with the scaling of the volume ratio. The changes in the model made in this work are described as follows. The values in Table 2 are used as the base parameters for the scaling.

Table 2: Expander model parameters and their values in Lemort et al. (2009)

$\alpha_\mathrm{amb}A_\mathrm{amb}$	$k_nA_\mathrm{su,L}$	$k_nA_\mathrm{ex,L}$	$\dot{m}_\mathrm{n}$	$A_\mathrm{leak,L}$	$\Pi_\mathrm{E,L}$	$V_\mathrm{s,exp}$	A_sup	$T_\mathrm{loss,L}$
W/K	W/K	W/K	kg/s	mm²	-	cm³	mm²	Nm
6.4	21.2	34.2	0.12	4.6	4.05	36.54	27.43	0.47

3.3 Scaling Method

Since the heat transfer between su, $1 \rightarrow$ su, 2 and ex, $1 \rightarrow$ ex is modeled as a solely convective heat transfer between the fluid and the fictitious isothermal envelope, it can be calculated with

$$kA_i = \alpha_i A_i. \tag{11}$$

To enable both the sizing of the geometry and the changing of the working fluid, the heat transfer coefficient will be calculated by means of a Nusselt-correlation

$$\alpha_i = \frac{Nu\lambda}{L_i}. \tag{12}$$

Equivalent to Lemort et al. (2009) the Nusselt number is calculated for a straight pipe and thus the Dittus-Bölter equation is chosen (Incropera et al., 2007)

$$Nu = 0.023Re^{0.8}Pr^{0.3}. \tag{13}$$

A well-chosen characteristic length L_su for the calculation of $\alpha_i = \alpha_\mathrm{su}$ is determined for the geometry of Lemort et al. (2008). The characteristic length L_ex is a function of the end involute angle and is calculated through

$$L_{ex} = L_{su}\sqrt{\Pi_E}. \tag{14}$$

The areas $A_{su,L}$ and $A_{ex,L}$ are calibrated on the model of Lemort et al. (2009), so that the area A_{su} can be calculated through

$$A_{su} = A_{su,geo}\frac{A_{su,L}}{A_{su,L,geo}}, \tag{15}$$

and A_{ex} through

$$A_{ex} = A_{ex,L}\frac{\Pi_E}{\Pi_{E,L}}. \tag{16}$$

The geometrical areas are calculated with the shell radius R_{sh} as $A_{i,geo} = \pi R_{sh}^2$ and $A_{i,L,geo}$ with the given parameters in Lemort et al. (2008). In general the shell radius is a function of the end involute angle and the governing equation can be found in Ma et al. (2017).

The friction force F_{Fr} between two bodies can be described by (Beater, 1999)

$$F_{Fr} = kv + \left(F_C + F_H e^{-c_1|v|}\right)sgn(v). \tag{17}$$

Since the scroll expander is an oil-free type, the viscous friction kv will be neglected. Therefore, if the relative velocity v between the bodies is sufficiently high, only the Coloumb force F_C needs to be considered

$$F_C = \mu \cdot F_N = \mu \cdot p_{con}S_N. \tag{18}$$

The force F_C multiplied with the lever arm R_{Or} results in a constant loss torque. These considerations align well with the measurements of an oil-free scroll expander in Yanagisawa et al. (2001). It showed that the mechanical loss torque was nearly independent of the rotational speed. To obtain a similar size of the clearances of the radial leakage paths in the scroll geometry during the scaling of the volume ratio of the expander, it is assumed that the contact pressure p_{con} between the scroll wraps and the base plates needs to remain constant. Under these considerations the following equation for the loss torque is received

$$T_{Loss} = 2S_{Scroll}p_{con}\mu R_{Or}. \tag{19}$$

The area S_{Scroll} describes herein the projected area of one scroll wrap on the base plate, calculated as shown in Ma et al. (2017). The value for $p_{con}\mu$ is calculated with the parameters in Table 2 and the geometry given in Lemort et al. (2008).

The geometrical leakage area for the scroll geometry is calculated as

$$A_{leak,geo} = A_f + A_r. \tag{20}$$

The area A_f describes the size of the flank clearance

$$A_f = \delta_f h_s, \tag{21}$$

the area A_r the size of the radial clearances. To receive an over one turn of the scroll wrap averaged value, the clearance length of a pocket is integrated over its lifetime ($\theta_{ex,end} - \theta_{su,0}$) and averaged

$$\bar{L}_r = \frac{1}{\theta_{ex,end} - \theta_{su,0}}\int_{\theta_{su,0}}^{\theta_{ex,end}} 2\pi a\theta \, d\theta = \frac{2\pi a\left(\theta_{ex,end}^2 - \theta_{su,0}^2\right)}{\theta_{ex,end} - \theta_{su,0}}. \tag{22}$$

The area A_r can now be calculated through

$$A_r = \delta_r\bar{L}_r. \tag{23}$$

Then the scaling is done with

$$A_{leak} = \frac{A_{leak,L}}{A_{leak,L,geo}}A_{leak,geo}. \tag{24}$$

Since this work is limited to the scaling of the end involute angle and thus the volume ratio, the inner area of the geometry of the expander scroll wraps is unchanged. Consequently, the suction volume and the area A_{sup} remain constant.

4   OPTIMIZATION PROCEDURE AND RESULTS

In this paper a collective optimization approach of the expansion machine and the thermodynamic points of state is carried out. The used optimization algorithm is the gradient based SLSQP-optimizer, as provided within the scipy library in python. At first, two different optimization procedures are carried

out. In both cases the expander model described in Chapter 3.3 is used, while the thermodynamic points of state p_3, h_3, p_1, and h_1 are optimized. In the first one, the parameters $A_{leak,L}$, $A_{su,L}$, $A_{ex,L}$, $T_{loss,L}$ and $\Pi_{E,L}$ of Table 2 are used, and thus the expander geometry remains unchanged and will be further called base expander. In the second case the volume ratio of the expander is also optimized through changing the end involute angle. The objective function of the optimization problem in all cases is Equation (1). The optimization takes place in a stationary exhaust gas state ($T = 350\,°C$, $\dot{m}_{ehx} = 0.2675\,kg/s$). Optimal control strategies are out of scope of this paper, as a consequence a fixed point has been chosen.

Table 3: Optimization parameters and results

	p_3	h_3	p_1	h_1	Π_E	η_{Exp}	η_{Ex}
	bar	kJ/kg	bar	kJ/kg	-	%	%
Constraints	≤ 45.71 (critical pressure)	≤ 850 always superheated	≥ 1	always subcooled	≤ 15	-	-
Base expander	17.90	603.9	1.77	16.90	4.05	70.05	26.91
Optimized expander	18.13	610.9	1.76	17.32	4.65	70.03	27.09

Table 3 shows the optimization constraints and also the results of the two optimization procedures like the exergetic efficiencies of the processes and the corresponding overall efficiencies of the expansion machine. The exergetic efficiency is defined as the net power output divided by the provided exergy flow of the heat source

$$\eta_{Ex} = \frac{\dot{W}_{res}}{\dot{E}}, \tag{25}$$

and the overall efficiency of the expander is calculated through

$$\eta_{Exp} = \frac{\dot{W}_{sh}}{(h_{4,Is} - h_3)}, \tag{26}$$

with the enthalpy $h_{4,Is}$ which would be reached if the expansion from state point 3 to 4 would be reversible. Figure 3 shows the essential state diagrams of the optimized expander. In Table 3 it can be seen that, after the optimization, there is no improvement of the overall expander efficiency and the increase of the exergetic efficiency is marginal, even though the volume ratio changes by more than 10 % compared to the base expander. This leads to the assumptions, that either the parameter set of the base expander is already close to the optimum, and/or that the result is dominated by the optimization of the process variables (p_3, h_3, p_1, and h_1)
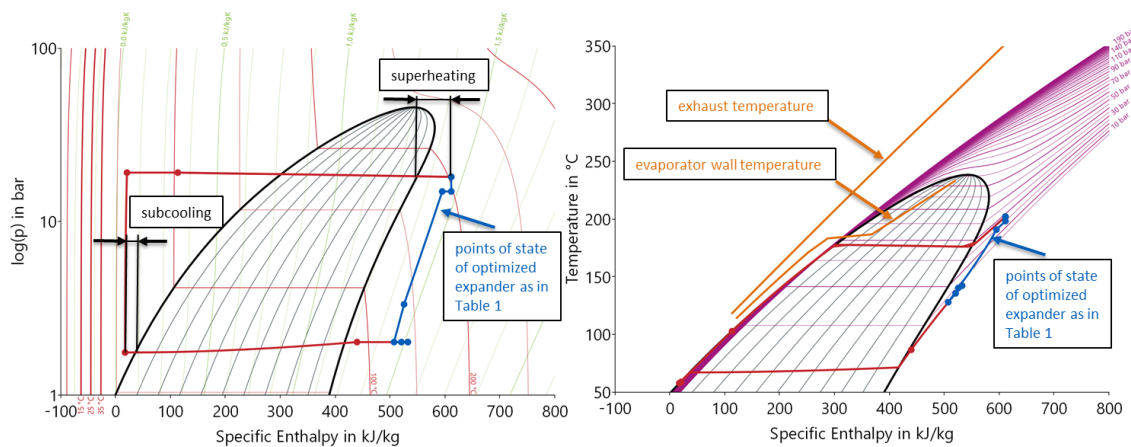

Figure 3: Log(p)-h-diagram (left) and t-h-diagram (right) of the final optimization result

In order to isolate this effect a two-step sensitivity analysis is carried out with respect to the volume ratio. In the first step, the optimized thermodynamic points of state are kept constant. The volume ratio is varied. The results are depicted in Figure 4 in blue. In the second step, the optimization problem for the thermodynamic points of state (p_3, h_3, p_1, and h_1) is solved while the volume ratio is varied. The results are depicted in Figure 4 in red. As one can see, the overall optimization result is, as expected, influenced by both the optimization of the thermodynamic points of state and the optimization of the geometric design of the expander. It shows that a poorly designed expander regarding to its volume ratio cannot be compensated by the optimization of the thermodynamic points of state. At a small distance to the ideal expander the exergetic efficiency of the process first drops slightly, but with rising deviation the losses increase noticeably. This leads to the realization that the origin parameters $A_{\text{leak,L}}$, $A_{\text{su,L}}$, $A_{\text{ex,L}}$ and $T_{\text{loss,L}}$ in Table 2 are close to the optimal volume ratio in consideration of the single given exhaust state. The small gradient of the exergetic efficiency in the area of the ideal expander leads the optimizer to a great change in the volume ratio with little influence on the exergetic efficiency. But if the expander is poorly designed a greater influence can be expected because of the sharply increasing losses with rising distance. It can be concluded that an optimization of the expander geometry should be included in addition to the optimization of the thermodynamic points of state. The modified expander model gives the option to do so. Still, this statement is the result of the examination of a single exhaust state and a more exhaustive investigation should be carried out in future works. Further is to say, that in a driving cycle of a long-range intercity bus the operation is highly dynamic and leads to highly transient operating conditions in the Rankine cycle. Thus, an optimal control design is needed. An influence of the optimal control design on the optimal design of the expander is assumed and should also be investigated.
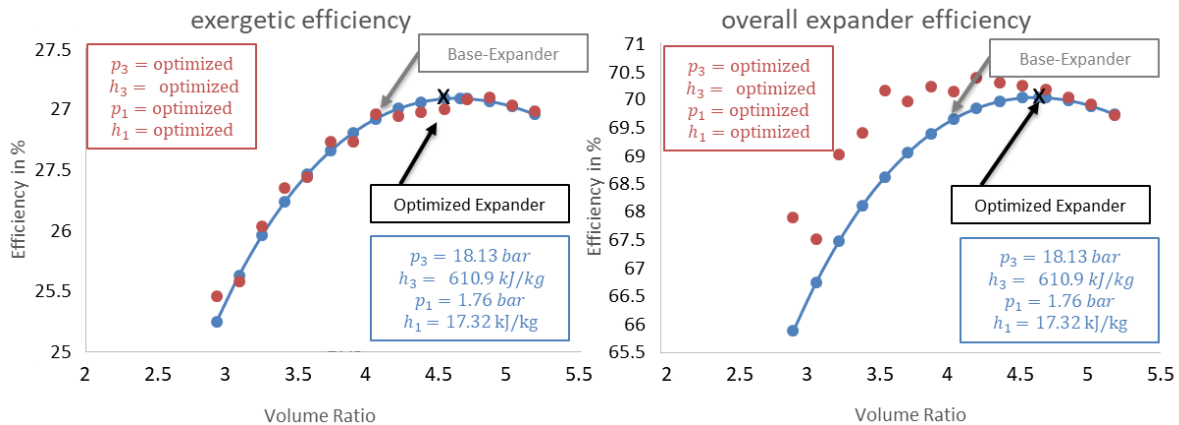

Figure 4: Results for the exergetic (left) and overall expander efficiency (right) in dependency of the volume ratio for optimized thermodynamics points of states in red and constant ones in blue

5   CONCLUSION

It is shown that the developed expander model with the ability of the scaling of the volume ratio works in the scope of a whole system optimization approach. The optimization of the expander geometry in addition to the optimization of the thermodynamic points of state shows potential and is highly recommended. The solely optimization of the points of states cannot outperform the combined optimization, especially if the expander has a poor design regarding to the boundary conditions.

NOMENCLATURE

$\dot{W}$	Power	W	**Subscript**	
$\dot{Q}$	Heat flux	W	res	Resulting
$\dot{m}$	Mass flow rate	kg/s	sh	Shell

Symbol	Description	Unit
$\dot{V}$	Volume flow	m^3/s
m	Mass	kg
V	Volume	m^3
p	Pressure	Pa
Δp	Pressure difference	Pa
h	Enthalpy	kJ/kg
s	Entropy	kJ/(kgK)
ϱ	Density	kg/m^3
T	Temperature	K
ϑ	Temperature	°C
A	Area	m^2
η	Efficiency	-
c	Spec. heat capacity	kJ/(kgK)
c_p	Isobaric c	kJ/(kgK)
kA	Thermal transmittance	W/m^2
$V_{s,exp}$	Suction volume expander	m^3
γ	Heat capacity ratio	-
T_{loss}	Loss torque	Nm
Nu	Nusselt number	-
λ	Thermal conductivity	W/m
L	Characteristic length	m
Re	Reynolds number	-
Pr	Prandtl number	-
F	Force	N
v	Velocity	m/s
μ	Coefficient of friciton	-
S	Surface area	m^2
R	Radius	m
δ	Leakage clearance	m
c_1	Decay coefficient	s/m
$\bar{L}_r$	Averaged radial leakage length	m
ϕ	Involute angle	rad
θ	Orbiting angle	rad
h_s	Height of scroll	m
α	Heat transfer coefficient	$W/(m^2K)$
$\dot{E}$	Exergy flow	W

Subscript	Description
p	Pump
amb	Ambient
f1 and f2	Fan 1 and 2
Is	Isentropic
su	Suction
sup	Suction port
thr,l	Throat leakage path
ad	Adiabatic
ex	Expansion
i	Subscript (position)
crit,leak	Critical Leakage
E	Expander
leak and l	Leakage
loss	Loss
in	Internal
w	Wall
L	Lemort
end or e	End
N	Normal
con	Contact
Or	Orbiting
geo	Geometrical
f	Flank
r	Radial
C	Coulomb
s	Scroll
H	Static
Ex	Exergetic
ehx	Exhaust gas

Abbreviations

SLSQP	Sequential Least Squares Programming Optimization Algorithm

6   REFERENCES

Ayachi, Fadhel; Ksayer, Elias Boulawz; Neveu, Pierre; Zoughaib, Assaad (2016): Experimental investigation and modeling of a hermetic scroll expander. In *Applied Energy* 181, pp. 256–267. DOI: 10.1016/j.apenergy.2016.08.030.

Beater, Peter (1999): Entwurf hydraulischer Maschinen. Modellbildung, Stabilitätsanalyse und Simulation hydrostatischer Antriebe und Steuerungen. Berlin, Heidelberg: Springer (VDI-Buch).

Fanelli, E.; Pinto, G.; Cornacchia, G.; Braccio, G. (2018): Parameters identification for scroll expander semi-empirical model by using genetic algorithm. In *Energy Procedia* 148, pp. 736–743. DOI: 10.1016/j.egypro.2018.08.140.

Incropera, Frank P.; DeWitt, David P.; Bergman, Theodore L.; Lavine, Adrienne S. (2007): Fundamentals of heat and mass transfer. 6. ed. Hoboken, NJ: Wiley.

Kaiser, Christian (2020): Untersuchungen zur Effizienz- und Leistungssteigerung von Omnibusklimaanlagen. Dissertation. Technische Universität Braunschweig.

Lemort, Vincent; Quoilin, Sylvain; Cuevas, Cristian; Lebrun, Jean (2009): Testing and modeling a scroll expander integrated into an Organic Rankine Cycle. In *Applied Thermal Engineering* 29 (14-15), pp. 3094–3102. DOI: 10.1016/j.applthermaleng.2009.04.013.

Lemort, Vincent; Quoilin, Sylvain; Lebrun, Jean (2008): Numerical Simulation of a Scroll Expander for Use in a Rankine Cycle. In : International Compressor Engineering Conference, Paper 1902.

Ma, Zhiwei; Bao, Huashan; Roskilly, Anthony Paul (2017): Dynamic modelling and experimental validation of scroll expander for small scale power generation system. In *Applied Energy* 186, pp. 262–281. DOI: 10.1016/j.apenergy.2016.08.025.

Panesar, Angad S.; Bernagozzi, Marco (2019): Two-Phase Expander Approach for Next Generation of Heat Recovery Systems. In *IJRED* 8 (3), pp. 203–213. DOI: 10.14710/ijred.8.3.203-213.

Winandy, Eric; Saavedra O, Claudio; Lebrun, Jean (2002): Simplified modelling of an open-type reciprocating compressor. In *International Journal of Thermal Sciences* 41 (2), pp. 183–192. DOI: 10.1016/S1290-0729(01)01296-0.

Wu, Zhu; Pan, Deng; Gao, Naiping; Zhu, Tong; Xie, Feibo (2015): Experimental testing and numerical simulation of scroll expander in a small scale organic Rankine cycle system. In *Applied Thermal Engineering* 87, pp. 529–537. DOI: 10.1016/j.applthermaleng.2015.05.040.

Yanagisawa, T.; Fukuta, M.; Ogi, Y.; Hikichi, T. (2001): Performance of an oil-free scroll-type air expander. In : International Conference on Compressors and their Systems, 9 - 12 September 2001, City University, London, UK. Bury St. Edmunds: Professional Engineering Publ. for The Institution of Mechanical Engineers (IMechE conference transactions, 2001,7), pp. 167–174.